Development of Zeeman Split-Assisted Tomography for Helium Line Emission Distribution in LHD

Tetsuto HARA[1)], Motoshi GOTO[2)], Kouji SHINOHARA[1)] and Satoshi OHDACHI[*]

[1)]*The University of Tokyo, Kashiwa 277-8561, Japan*

[2)]*National Institute for Fusion Science, Toki 509-5292, Japan*

(Received 5 October 2023 / Accepted 17 December 2023)

We have measured the emission line spectra of neutral helium ($2^1P - 3^1D$, 667.8 nm) in a poloidal cross-section of the plasma in the Large Helical Device (LHD). The measurement has been made from two different observation ports with 40 lines-of-sight each. A tomographic analysis was done to derive the line intensity distribution, using the Hopfield Neural Network method with the Phillips-Tikhonov regularization term. The algorithm was expanded to incorporate Zeeman splittings, a feature prominently evident in the measured spectra, providing information on the position of the emission. The results revealed a concentrated radiation distribution near the X-points and on the divertor legs, specifically those connected to the inboard side divertor plates. We have confirmed that reconstructed images are available even when the analysis is performed solely with data from one of the two observation ports. This suggests the potential applicability of our approach under highly limited options for observation port arrangements. By reconstructing the line emission distribution only using the π peak signals, we show that our method can estimate the vertical emission positions from the Zeeman effect. The robustness of our new method was also checked.

Keywords: sparse-data tomography, Zeeman effect, plasma imaging, LHD

DOI: 10.1585/pfr.19.1402009

1. Introduction

In deuterium-tritium fusion, low-energy helium, or helium ash, should be removed from the confined plasma. Therefore, understanding helium transport is an important research topic. For this purpose, the behavior of neutral helium should be investigated.

The main source of neutral helium in the plasma boundary region is recycling in the divertor, and a complex density distribution is expected [1]. Therefore, the measurement of helium atom distribution is important to study the particle control for better confinement on general toroidal plasmas. However, it is generally difficult to determine the atom density distribution in the vacuum region far from the Last Closed Flux Surface (LCFS). This is because neutral atoms are not excited and do not emit electromagnetic waves, so there is no clue to determine their density distribution.

In regions where neutral atoms enter the plasma, atoms radiate emission lines mainly due to excitation, and their intensities can be determined from spectroscopic measurements. Since the intensity of the emission lines represents the atom influx toward confined plasma, if the poloidal distribution of line intensities is obtained, they provide us a clue to know the neutral helium density distribution at the plasma periphery.

What we can measure are generally line-integrated emission intensities. Therefore, it is natural to consider using a tomographic technique [2, 3] for reconstructing the local emission distribution. In the Large Helical Device (LHD), however, due to the limitation of the port locations, it was not possible to observe a poloidal cross-section with arrays of lines-of-sight from largely different directions. Furthermore, neutral atoms are not trapped in a magnetic field, so it is not possible to use a tomographic technique that supposes a uniform density on the magnetic surface, as is the case with ions. Therefore, it was difficult to conduct conventional tomographic analyses for the measured neutral atom line intensity data.

The measured signal g_m at the wavelength λ is the line-integral of Zeeman spectrum Z at position $\boldsymbol{r}$ multiplied by emission intensity $\boldsymbol{f}$ on the line-of-sight index m. That is

$$g_m(\lambda) = \int_m Z(\lambda, \boldsymbol{r}) f(\boldsymbol{r}) d\boldsymbol{r}. \quad (1)$$

Goto and Morita have tried to determine the emission positions from line-integrated measured spectra $g_m(\lambda)$. They took advantage of the fact that the measured spectra show the Zeeman split, which has the information on emission positions through the magnetic field strength. They used a least squares method to reconstruct the emission distribution image based on two assumptions. First, helium neutrals can emit light only at the plasma periphery and at the divertor legs. Second, emissions are localized at several

author's e-mail: hara-tetsuto@g.ecc.u-tokyo.ac.jp

[*] *deceased in 3/26/2023*

points on the line-of-sight. Namely, they solved

$$\underset{A,\boldsymbol{r},\boldsymbol{v}}{\operatorname{argmin}} \sum_i \left\| g_i(\lambda) - \sum_{j=1}^{2} A_j G_j(\lambda; \boldsymbol{r}, \boldsymbol{v}) \right\|^2, \tag{2}$$

where A is emission intensity, G is the Zeeman spectrum calculated at position $\boldsymbol{r}$ and atom velocity $\boldsymbol{v}$, $g_i(\lambda)$ is the measured spectrum of line-index i. Although the reconstructed image was reasonable in many respects from a physical point of view, there were two problems: 1) There are generally two points that have the same magnetic field strength on a single line-of-sight due to the convex structure of the magnetic field strength. As a result, the emission location could not be completely identified. Areas where there is no plasma and no source to excite neutral helium atoms were selected as the emission locations by the algorithm. Such emission locations are hereafter called ghosts. 2) Because line emissions were assumed to be localized, it was not possible to know the spatial extension of emission regions in the reconstructed image.

In this research, we have developed a tomography method that can determine the emission distribution under a limitation regarding the observation direction. The new tomography method utilizes Zeeman split spectra which have information on longitudinal emission positions along a line-of-sight and assumes that emission distribution is spatially smooth and has no negative values [4, 5].

2. Experimental Setup

The data used in this research are measured spectra for the LHD shot number 47518 [1]. As shown in Fig. 1, 40 lines-of-sight from two different ports are used to measure a poloidal cross-section of the LHD plasma. Spectroscopic measurements have been made with a spectrometer shown in Fig. 2 (a). The light focused on the fiber is introduced into the pre-optics and then enters the entrance slit of the spectrometer. The light diffracted by the grating is then recorded with a CCD (Charge-Coupled Device) camera. The curved slit in Fig. 2 (b) and the pre-optics in Fig. 2 (a) are tailored to compensate the astigmatism [1].

Figure 2 (c) shows an example of CCD images for the hydrogen Balmer α line. The horizontal structure is due to the Zeeman effect and the Doppler broadening, and the vertical direction corresponds to different lines-of-sight in Fig. 1. As shown in Fig. 2 (b), the entrance slit is curved, which causes the image on the CCD camera to be curved as shown in Fig. 2 (c).

The actual measurement was made for a helium singlet line $2^1\mathrm{P} - 3^1\mathrm{D}$ which shows the normal Zeeman effect by a magnetic field, i.e., the spectrum consists of one unshifted π-light and two symmetrically shifted σ-lights. Nevertheless, observed spectra sometimes give more than three peaks as shown in Fig. 3. This spectrum can be regarded as a superposition of two Zeeman split spectra emitted at two positions having different magnetic field strengths. The details will be discussed later.

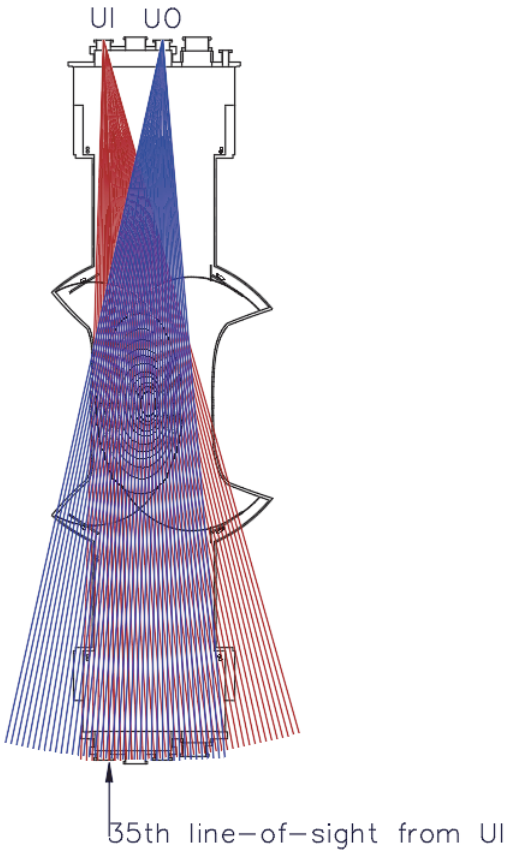

Fig. 1 Two groups of lines-of-sight for spectroscopic observations. The port on the upper outboard side is referred to as UO and the port on the upper inboard side as UI.

It is noted that we have calibrated the wavelength axis for each line-of-sight using a recombining plasma observed at the end of the discharge for which the Doppler broadening and shifts are expected to be negligibly small.

We also note that when θ is defined as the angle between the line-of-sight and the magnetic field, the intensities of π- and σ-lights, I_π and I_σ, respectively, can be expressed as [6]

$$I_\pi = \frac{1}{2} I_0 \sin^2\theta, \tag{3}$$

$$I_\sigma = \frac{1}{4} I_0 (1 + \cos^2\theta), \tag{4}$$

where I_0 is the total intensity. The distribution of the magnetic field strength for this research is shown in Fig. 4. Therefore, the ratio of π- and σ-light intensities have information on the angle between the line-of-sight and the magnetic field.

A conceptual diagram that indicates the measured data are superposition of Zeeman spectra along each line-of-sight (Eq. (1)) is shown in Fig. 5. Figure 5 (a) assumes uniform emission distribution on the magnetic field lines toward the divertor plates based on previous research [1]. The red line is the 35th line-of-sight of the UI port in Fig. 1.

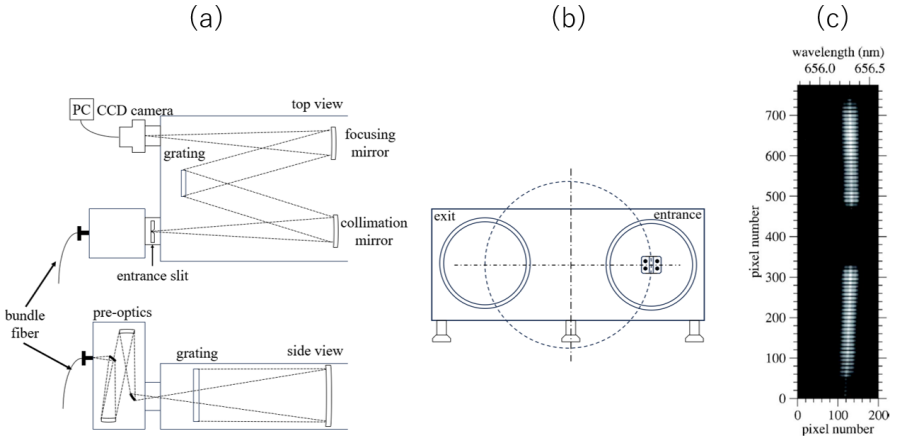

Fig. 2 (a) Schematic drawing of the spectrometer, (b) curved entrance slit for correcting an aberration, (c) spectral images on the CCD for the Balmer α line of neutral hydrogen. The slit image on the CCD camera is curved due to the curved slit.

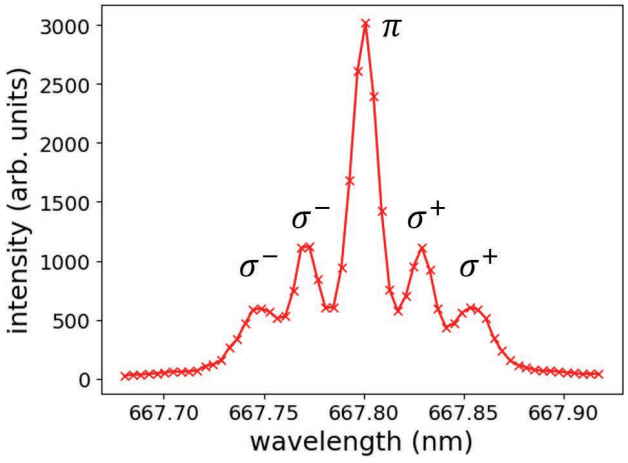

Fig. 3 Example of measured spectra of the helium $2^1P - 3^1D$ line. This spectrum is understood as a superposition of multiple Zeeman split components. The central peak is the overlapped π-lights and other peaks are σ-lights of individual components.

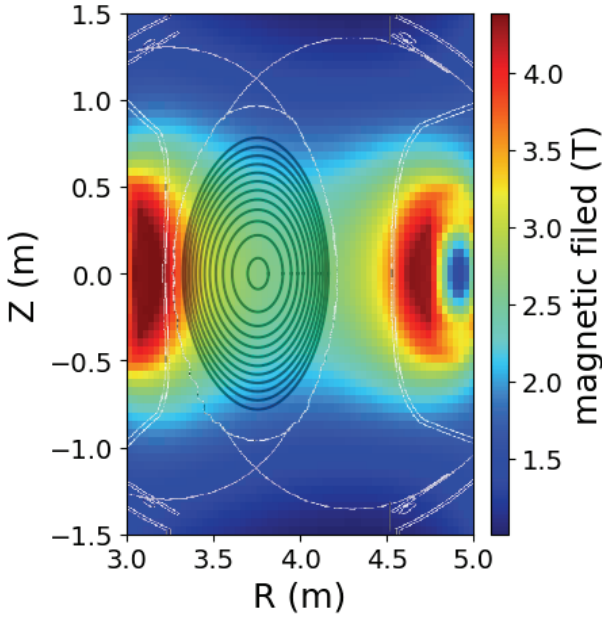

Fig. 4 Magnetic field strength distribution in the poloidal cross-section observed in this research.

Figure 5 (b) shows the Zeeman split spectra at the blue and red points in Fig. 5 (a) calculated with the magnetic field strength distribution in Fig. 4. Figure 5 (c) shows the synthetic spectrum integrated over the line-of-sight. It is noted that the spectrum does not include the component of 3.38 T because no emission is assumed at this point.

3. Methodology

3.1 Tomography

The tomography technique is a method of reconstructing distributions from line-integrated data. We treat signals at different wavelengths as independent measurements (input for tomography) hoping that the problems in the previous research are solved. There are two reasons to expect that. First, the tomography method can reasonably determine the emission of a certain cell by using the information possessed by multiple lines-of-sight data. In this research, measured data have positional information in the wavelength separation of the π peak and σ^+, σ^- peaks and in the intensity ratio of the I_π and I_σ due to the Zeeman effect, which depends on the magnetic field. Therefore, it is expected that the information of the magnetic field along the line-of-sight will be reflected in the reconstructed image by using the tomography method. Second, since the assumption of an emission region is not necessary, the emission distribution over the entire area can be obtained. The first reason will be discussed in more detail in Sec. 3.3.

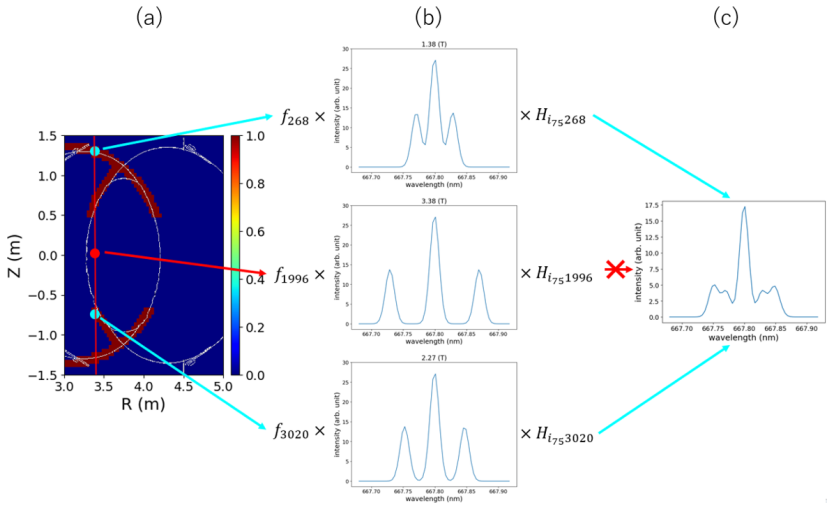

Fig. 5 Conceptual diagram explaining that the measured spectra are the superposition of different shapes of Zeeman spectra along the line-of-sight. The red line indicates the 35th line-of-sight from UI port in Fig. 1. (a) Test image assuming emission on the magnetic field lines toward the divertor is of uniform emission intensity, (b) Zeeman spectra at the positions indicated by the dots in (a), (c) artificial measured spectrum created from the test image (a). The artificially measured spectrum is formed by line integrals of emission points along the line of sight, not just the two representative points indicated by the blue dots (a).

3.2 Tomography formulation

The line-integrated intensity of the line-of-sight m, g_m, can be expressed as

$$g_m = \int_D h_m(\boldsymbol{r}) f(\boldsymbol{r}) d\boldsymbol{r} + \epsilon_m \,, \tag{5}$$

where $\boldsymbol{r}$ stands for the position, $f(\boldsymbol{r})$ is the emission intensity distribution on the target area D, and $h_m(\boldsymbol{r})$ is the contribution function. The line-of-sight index m runs from 1 to M. Data generally includes noise which is here represented by ϵ_m. The region of interest is divided into a total of K cells, and discretizing the above equation yields

$$g_m = \sum_{k=1}^{K} h_{mk} f_k + \epsilon_m \quad \rightarrow \quad \boldsymbol{g} = H\boldsymbol{f} + \boldsymbol{\epsilon}. \tag{6}$$

Here, the matrix elements h_{mk} represent the contribution times the path length elements for a line-of-sight m and for a cell k. Generally, the total number of cells K is much larger than the total number of lines-of-sight M due to limited observation port arrangement, that is $M \ll K$, and the matrix H has no inverse matrix. Therefore, we define the following loss function $\Lambda_\gamma(\boldsymbol{f})$ as

$$\Lambda_\gamma(\boldsymbol{f}) = \gamma P(\boldsymbol{f}) + \frac{1}{M} \|H\boldsymbol{f} - \boldsymbol{g}\|^2, \tag{7}$$

and seek $\boldsymbol{f}$ that minimizes this loss function, where P is the regularization term and γ is the parameter that controls the regularization term contribution, $\|\cdots\|^2$ indicates the L2 norm of the given vector.

3.3 Utilization of Zeeman splitting

In the tomographic method formulated in Sec. 3.2, the data for each line-of-sight is supposed to be a line-integrated intensity, which is a scalar quantity. However, the measured data in this case is the spectrum of a Zeeman-split emission line, which depends on the magnetic field strength and direction. In order to treat the spectrum with the conventional tomography method, let $\boldsymbol{g}$ be a one-dimensional vector of the intensities of all the points that compose the spectrum for all the lines-of-sight. Figure 6 explains how g_{m_i}, which is an element of $\boldsymbol{g}$, is constructed.

The Zeeman splitting is obtained by solving the Schrödinger equation with a perturbed Hamiltonian. The $2^1\mathrm{P} - 3^1\mathrm{D}$ spectrum of helium Zeeman split line can be calculated from the magnetic field distribution as shown in Fig. 4, and the spectral data $Z_{m_i k}$ along the line-of-sight can be prepared as shown in Fig. 7. When calculating the Zeeman split spectrum, the Doppler shift is taken into account by supposing the velocity of the helium neutral atom to be v_{helium} ~2000 m/s in the direction normal to the LCFS following Ref. [7]. The Doppler broadening is also given assuming that the helium atom temperature is T_{helium} ~300 K also following Ref. [7].

The redefinition of the matrix H as described in Fig. 6 creates two advantages for solving the problem. First, since the wavelength separation due to the Zeeman split depends on the magnetic field strength, positional information can be added to the tomographic method. Second, the number of rows of the matrix H is increased so that the $M \ll K$ condition becomes somewhat milder. Each spectrum consists of 1024 points, and we choose non-trivial 60 points centered at the π component of the Zeeman-split spectrum. In this case, the number of rows in the H matrix is a multiplication of the number of points that make up the spectrum and the number of lines of sight, so that $60 \times 80 = 4800$.

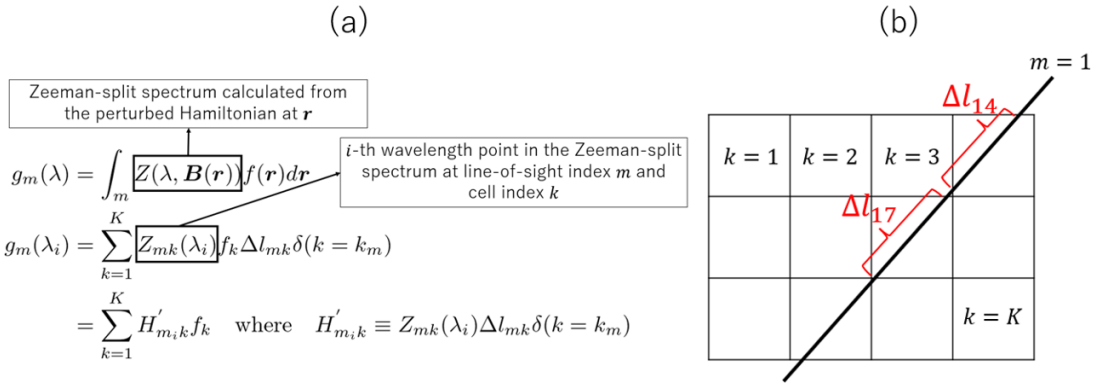

Fig. 6 (a) Formulation of a tomography method using the Zeeman spectrum. $\delta(k = k_m)$ only picks up cells along the line-of-sight. (b) Diagram of Δl_{mk} for line-of-sight index $m = 1$. Δl_{mk} is the line element when the line-integral is discretized. It is approximated by the length that line-of-sight m cuts a cell k.

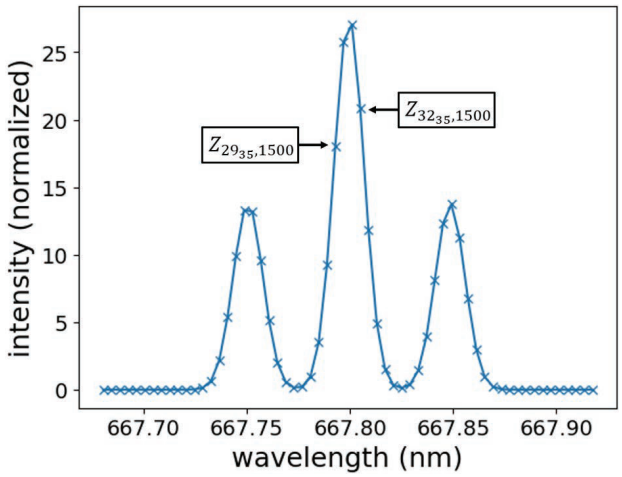

Fig. 7 Zeeman spectrum calculated at cell index 1500, magnetic field strength 2.35 T, assuming the angle θ that is formed by line-of-sight and magnetic field is $\pi/2$. $Z_{29_{35}1500}$ and $Z_{32_{35}1500}$ are specific value examples in Fig. 6.

3.4 Adopting developed tomography method for measured data

Phillips-Tikhonov regularization, where $P(\boldsymbol{f}) = \|\Delta \boldsymbol{f}\|^2$ in Eq. (7), is employed as the regularization term since the distribution of the emission intensity should be continuous [4]. The operator Δ is a discretized representation of the Laplacian. In addition, since the emission intensity is non-negative, Hopfield Neural Network (HNN) [5], which requires the condition of non-negative intensity $\boldsymbol{f}$, was employed as the reconstruction method.

The regularization parameter γ is determined by the L-curve as shown in Fig. 8, which is a plot of $\|\Delta \boldsymbol{f}\|$ against $\|H\boldsymbol{f} - \boldsymbol{g}\|$ [8]. There are two major stances of determining γ: the first is that γ is chosen just at the point where the side constraint $\|\Delta \boldsymbol{f}\|$ and the residual norm $\|H\boldsymbol{f} - \boldsymbol{g}\|$ are in balance; the second is that γ is taken to reduce the residual norm, namely in order to "squeeze out" more information from the measured data [8]. So, the former corresponds to taking the regularization parameter at the "corner"of L-curve, and the latter corresponds to taking the regularization parameter on the slightly left side of the "corner". Here, we chose $\gamma = 5.30 \times 10^{-12}$, where the residual norm begins to grow near the "corner".

4. Results and Discussion

Figure 9 shows the results of tomographic analysis for the measured spectra using the method described in Sec. 3. The emission at the plasma boundary is understood as the location where neutrals are dominantly excited and emitting light. The emissions on the divertor legs are expected to be the result of the plasma heading to the divertor colliding and exciting neutrals and causing them to emit light.

The magnetic field structure of LHD is symmetric with respect to the $Z = 0$. However, the reconstructed emission distribution has asymmetry. This might be due to the asymmetric experimental setup or asymmetric dynamics of the divertor heading plasma. Further research is needed to explore the reasons in detail.

By supplementing the vertical position information from the Zeeman splitting, the reconstructed image was successfully obtained. As a result, one of the two problems mentioned in Sec. 1 is solved: The emission intensity is obtained as a distribution and not as several local positions in the target area. Although, ghost emission intensity on the lower right area becomes smaller, it has not disappeared completely. The reason for the ghost is thought to be due to the insufficient wavelength resolution of the spectrometer which determines the resolution of the magnetic field strength derived from the spectra. The ghost might be suppressed by using a spectrometer with a higher wavelength resolution.

Figure 10 shows the reconstruction of the emission intensity distribution using the measured data only from the UI or UO port. In both cases, results are similar to that using the measured data from both the UI and UO ports.

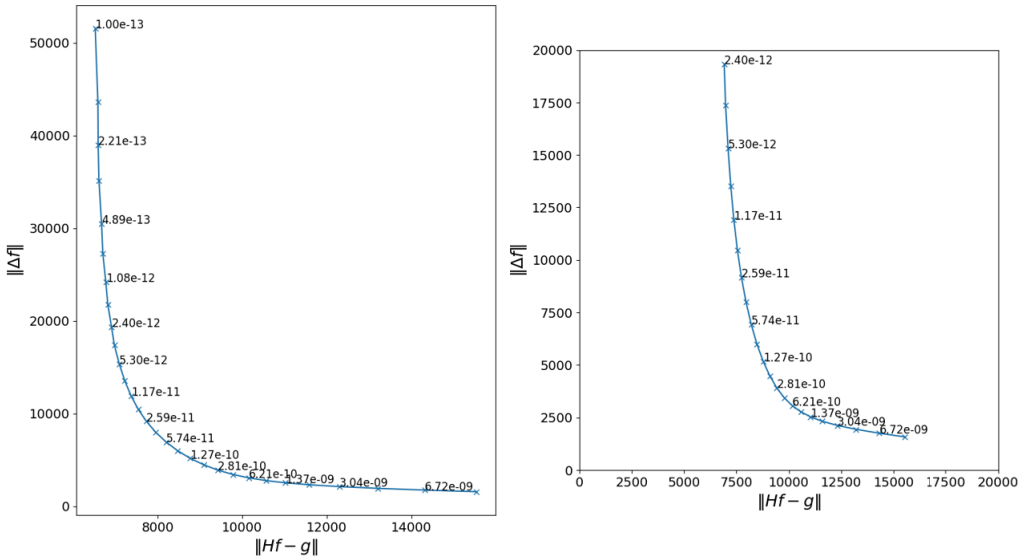

Fig. 8 (a) L-curve drawn with regularization parameter γ from 10^{-13} to 10^{-9}. (b) Replot of (a) with equal scales for both axes around the "corner".

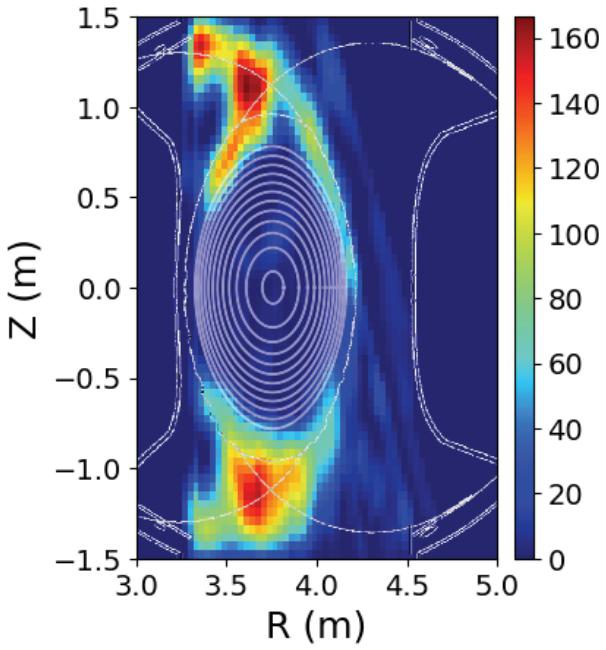

Fig. 9 Reconstructed helium line intensity distribution image using all the UO and UI port data.

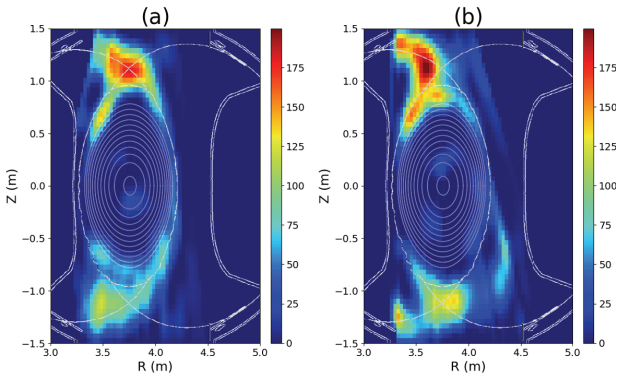

Fig. 10 (a) Reconstructed emission distribution using only the UO port measured data in Fig. 1. (b) Reconstructed emission distribution using only the UI port measured data in Fig. 1. Both images were reconstructed by HNN, and in both cases, the regularization term was set to $\gamma = 2.40 \times 10^{-12}$. Although the image is blurred compared to Fig. 9 which uses the lines-of-sight that overlap, the tomography algorithm is still able to estimate the vertical emission position from the Zeeman splitting.

This result suggests a possibility to do a tomographic reconstruction with a single set of lines-of-sight by utilizing the Zeeman effect when the observation port arrangement is further limited.

The image reconstruction was attempted using only the π component of the Zeeman spectrum to confirm that the wavelength separation of the Zeeman split adds positional information to the tomography technique. The reconstruction result is shown in Fig. 11. The regularization parameter $\gamma = 1.44 \times 10^{-10}$ was chosen, considering the dependence of the mean squared error $\epsilon^2 = (1/M)\|\boldsymbol{Hf} - \boldsymbol{g}\|^2$ and the L-curve on γ. The reconstructed emission distribution became totally unreasonable which indicates that it is hard to retrieve information on the longitudinal emission positions since the two groups of the lines-of-sight, the UI and UO groups, are nearly parallel.

Finally, to demonstrate the robustness of the reconstructed image against the initial guess image, reconstruction calculations were done from several initial values. The results are shown in Figs. 12 to 14, which demonstrate the robustness of our method.

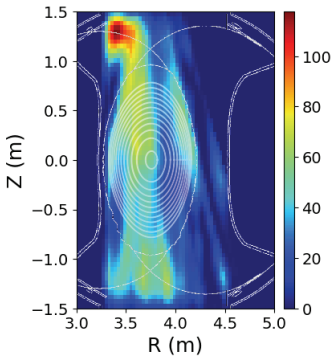

Fig. 11 Emission distribution reconstructed using only the π component of the Zeeman split.

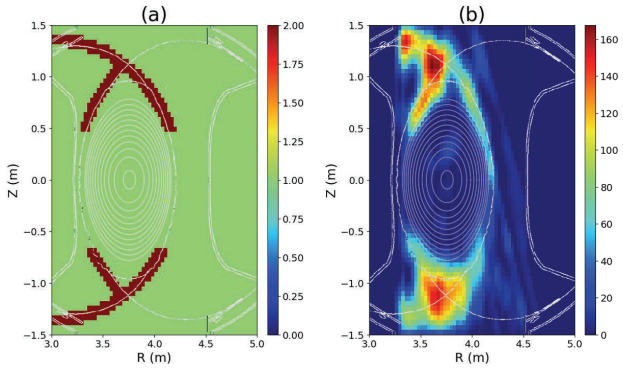

Fig. 12 (a) Initial image for HNN. Assuming emission on the magnetic field lines. (b) Emission distribution reconstructed from the initial image (a).

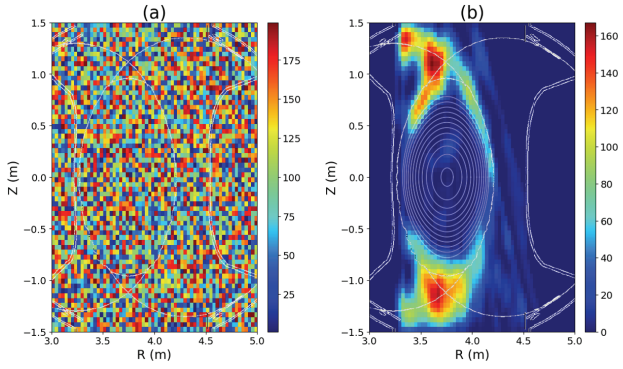

Fig. 13 (a) Initial image for HNN. Assuming a random integer between 1 and 200 for each cell. (b) Emission distribution reconstructed from the initial image (a).

5. Summary

We have developed a new tomography method that incorporates the Zeeman effect which has the positional information of emissions. The Hopfield Neural Network (HNN) method with the Philips-Tikhonov regularization term was selected as a tomography algorithm. Adopting this new method for the measured data, even with the lack

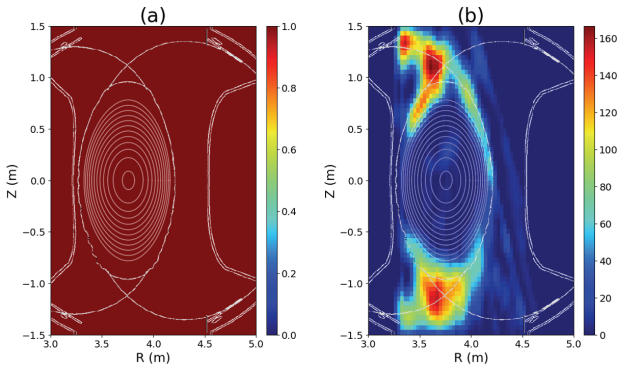

Fig. 14 (a) Initial image for HNN assuming a flat distribution. (b) Emission distribution reconstructed from the initial image (a).

of horizontal lines-of-sight the vertical emission position was estimated from Zeeman splitting wavelength width and the angle between the line-of-sight and the magnetic field. The reconstructed helium atom line emission distribution indicates a concentrated radiation distribution near the X-points and on the divertor legs, specifically those connected to the inboard side divertor plates. Satisfactory results were obtained even from the measured data of the single port lines-of-sight group. This result suggests this new method can be used under high port limitation conditions, such as in future devices. It was checked that the Zeeman effect added vertical location information to the tomographic method by reconstructing the emission distribution using only the measured data π peak intensities. By attempting the HNN calculation from several initial conditions, the robustness of the HNN was also confirmed. As future works: 1) Another regularization term should be checked to see whether we can get a better reconstruction image. 2) The reason for the asymmetry structure of the reconstructed image should be investigated. 3) It should be tested whether higher wavelength resolution spectrometer data would further clarify helium atom line emission distribution.

Acknowledgments

We wish to thank Seki Ryosuke at National Institute for Fusion Science for providing the FORTRAN code and server to calculate the magnetic field distribution and for his various advice. The authors are grateful to Munechika Koyo at Tokyo Institute of Technology for his various advice on tomography. We have learned a great deal from his library CHERAB-PHiX, a library for sparse-data tomography in nuclear fusion field, and its documentation. We would like to thank Inagaki Shinichiro at Kyoto Institute of Technology for his various advice on tomography method. We are grateful to Simons Joseph John of The Graduate University for Advanced Studies, SOKENDAI. He gave us the careful correction of our manuscript.

[1] M. Goto and S. Morita, Rev. Sci. Instrum. **77**, 10F124-1 (2006).
[2] S. Ohdachi *et al.*, J. Plasma Fusion Res. **14**, 3402087 (2019).
[3] Y. Nagayama, J. Appl. Phys. **62**, 2702 (1987).
[4] N. Iwama *et al.*, Appl. Phys. Lett. **54**, 502 (1989).
[5] N. Iwama *et al.*, J. Plasma Fusion Res. SERIES **8**, 691 (2009).
[6] M. Goto, *Plasma Polarization Spectroscopy*, eds. T. Fujimoto, A. Iwamae (Springer, Berlin, 2008) p.13.
[7] M. Goto and S. Morita, Phys. Rev. E **65**, 026401 (2002).
[8] P.C. Hansen, Inverse Problems **8**, 849 (1992).